Improving Human-Robot Object Exchange by Online Force Classification

Wuwei He, Daniel Sidobre

Improving Human-Robot Object Exchange by Online Force Classification

Wuwei He and Daniel Sidobre
CNRS, LAAS, 7 avenue du colonel Roche, F-31400 Toulouse, France
Univ de Toulouse, UPS, LAAS, F-31400 Toulouse, France

April 2015

abstract

Handing an object over to a human is a challenging task for a robot to perform, especially when the human partner has no experience interacting with robots. This paper presents our work to enable a robot to learn how to achieve this task with wrist force/torque sensing. Firstly, we present a device to record the data, then we discuss the techniques used for the teaching. We choose to focus on the classification problem defined to enable the robot to find the finger opening movement. The main challenge is that the classification should be run online, at a comparable rate to the controller. To achieve a computationally efficient classifier, the Wavelet Packet Transformation is used for feature extraction, and then we used the Fisher criterion to reduce the dimension of features. A Relevance Vector Machine is used for the continuous classification procedure mainly for its sparsity. Some recorded data and the results from dimension reduction are shown, then we discuss the accuracy and sparsity of the classification by Relevance Vector Machine in this application. The software of continuous classification on forces is then tested on the robot for interactive object exchange between human and robot, which gives promising results.

keywords: Robotic, Physical interaction, Object exchange, Relevance Vector Machine

1 Introduction

The exchange of objects between human and robot is one of the elementary tasks that an interactive mobile manipulator has to perform. Either in the daily life or in the industrial contexts, natural and intuitive object exchange is preferable for the human partner. To achieve this goal, a device is proposed to teach robots the ability to exchange objects naturally as the humans do.

To achieve safe object hand-over, one of the important challenges for the robot is to determine if it is safe to open the fingers, and the right moment to open the fingers.

In this paper, we show how to learn this skill from force signals recorded by an instrumented device during object exchange between people. This device, named Bidule, uses a 6D force/torque sensor to record interaction forces during the exchanges. We model this force signal in classes that we identify by classification techniques based on a Relevance Vector Machine applied to the information extracted from the force signal. The underlying objective is to identify information that is useful to people during human to human hand-over tasks.

In order to detect grasping, we use wavelet analysis and classification techniques to study object exchange between people. We also propose solutions to reduce the dimension of the classification model. This model, learned from human experience, is then used to teach the robot the capability to know if the human has grasped the manipulated object and to decide when to react.

We present first experimental results obtained with our robots at *LAAS-CNRS* implementing a full exchange task that integrates the results from human aware motion planning, trajectory generation and control, and safety issues such as online collision checking and external force monitoring on robot joints (Sidobre et al., 2012).

The objective of this paper is to present the object designed and the set of techniques used to extract efficiently patterns from the force signals during object exchange. Even if it is still a primarily study, we show the possibility of learning a model from force signals during human interaction aiming to improve physical Human Robot Interaction. We paid a particular attention to choose efficient tools to build our demonstrator and show the capacities of the approach to extract the relevant information from the transmitted force, and so enhance object exchanges.

Related works are presented in Section 2. The Bidule object, designed to study the interaction forces during exchange, is presented in Section 3. The main part of the paper is Sections 4 and 5, which explain the techniques for feature extraction and classification. Then we give some results obtained with a robot in Section 6, followed by the conclusion.

2 Related Work

A solution to exchange objects between a human and a four-fingered robot hand was presented in (Nagata, Oosaki, Kakikura, & Tsukune, 1998). Authors used a 6-axis force/torque (f/t) sensor mounted on each fingertip to control the grasping force and evaluate modifications in human grasp condition. Similarly, in the domain of cooperative manipulation with humans (Aggarwal, Dutta, & Bhattacharya, 2007; Takubo, Arai, Hayashibara, & Tanie, 2002), researchers try to detect the different stages of cooperation like contact and slip.

The study of forces during object exchange can be done with a sensorized object (Kim, Nakazawa, & Inooka, 2002; Nakazawa, Kim, Inooka, & Ikeura, 2001; Nakasawa, Kim, Inooka, & Ikeura, 1999). Their object was designed to be grasped by two fingers, which are the thumb and the forefinger so the forces are only measured in two directions. When they designed the object, they proposed to answer a set of questions. The same questions can define the objective of our learning based approach too:

- "How does the giver know the receiver's contact?"
- "Which one starts to act first for the smooth hand-over?"
- "How do both of them control the grasp forces during the hand-over?"

And they established that "the giver may feel slight vibrations on the fingertip and a change in the weight of the object as the receiver contacts the object". They also showed that the grasp forces are adapted to the weight of the object.

A recent work using a sensorized baton to teach a Willow Garage PR2 robot demonstrates the validity of the approach (Chan, Parker, Van der Loos, & Croft, 2013). The authors built four controllers from the results of a study on human-human hand-overs using the baton. Then they asked participants to compare the controllers. The results show that the controller directly derived from learned elements is the one preferred by participants. But, the conclusion of the paper states that the tests were limited to one object exchanged in a vertical orientation. As the manual construction of a general controller will be very tedious, we propose here to use analysis and classification tools. Likewise the measure of the grasping force is difficult in the general case, in (Chan et al., 2013) a particular grasp corresponding to the position of a Force Sensitive Resistor sensor is used. In our case, the robot does not control the grasp force and simply open the fingers of the gripper, so the users can use more natural and varied grasps.

Another important consideration is related to the localization of the information in both time and frequency domains. *Vibration* condition, defined as a threshold on the high-frequency hand acceleration signal, can be used to detect the contact with environment when the robot places an object (Romano, Hsiao, Niemeyer, Chitta, & Kuchenbecker, 2011). Here again, the threshold is determined by manual trial and error, which would be especially difficult when multiple types of contact should be classified.

The methods used in this paper are wavelet analysis based. Readers can refer to (Mallat, 2008) for a detailed discussion on wavelets and the comparison to Fourier analysis and its variants. The Linear Discriminant Analysis is used to select features, a nice explanation of which can be found in the book (Bishop et al., 2006). Relevance Vector Machine, used as a classifier in this work, was firstly introduced in (Tipping, 2001). Frequency information based classification, although with different feature formation, is also reported with successful application on touch classification (Sato, Poupyrev, & Harrison, 2012), and especially on image classification, such as (Rehman, Gao, Wang, & Wang, 2012).

3 Bidule: a Device for Manipulation Learning

The first objective of this research was to design an autonomous object being able to record contact forces and motion. We designed an object, called Bidule, to learn useful information during object exchange like force and motion signals. The goal is that the learned information can be directly used on robots equipped with a wrist f/t sensor. The f/t sensor is common for mobile manipulators and for robots without a f/t sensor, the wrist f/t can be often estimated. The device was also designed to help to learn the

trajectories and the force control policies, however the details of these last two parts will not be covered in this paper.

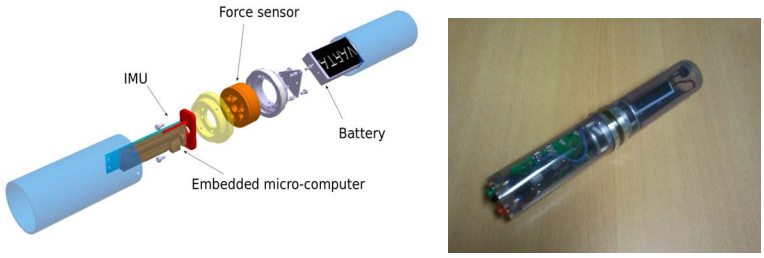

Figure 1: Left: Bidule design with the 6D force/torque sensor (orange), the handle (blue) are fixed on rings screwed to the sensor, the computer is on the left side and the battery with the power supply board on the right side. Right: Bidule, the device used during this research.

Bidule is built up around an embedded Gumstix microcomputer, a WiFi link, and a 6D force/torque sensor. An Inertial Measurement Unit (IMU) is used to compensate inertial forces and to record the motions of Bidule. The shape and the size were designed to fit better the human hand (Figure 1). Two tubes can be grasped by humans and transmit the external forces to the sensor.

The force signals are amplified, filtered and re-scaled before an Analog to Digital Converter (ADC) digitizes these signals. The link between the computer board and the acquisition board is done via a SPI link running at 3M bits/s available on a 60 pins connector. Two additional bronze rings, each of mass 0.227 kg, can be added around the Bidule object of mass 0.529 kg. This enables us to study different exchange forces when the mass of exchanged objects varies.

During manipulation, the f/t sensor records not only the contact forces of Bidule with the environment, but also the inertia of Bidule. Dynamic compensation needs to estimate firstly the inertial parameters (the mass, center of mass, and all elements in the inertia matrix) of the upper and bottom parts of Bidule. This problem can be illustrated by Figure 2. The whole set of inertial parameters of the upper part of Bidule is named $\boldsymbol{G}_1$:

$$\boldsymbol{G}_1 = (m \;\; c_x \;\; c_y \;\; c_z \;\; I_{xx} \;\; I_{xy} \;\; I_{xz} \;\; I_{yy} \;\; I_{yz} \;\; I_{zz})^T \tag{1}$$

Where m is the mass of this part, vector $(c_x \;\; c_y \;\; c_z)^T$ represents the position of the center of mass in the frame F_S of the force sensor and $(I_{xx} \;\; I_{xy} \;\; I_{xz} \;\; I_{yy} \;\; I_{yz} \;\; I_{zz})^T$ includes all the terms in the inertial matrix I, which can be written as:

$$\boldsymbol{I} = \begin{bmatrix} I_{xx} & I_{xy} & I_{xz} \\ I_{xy} & I_{yy} & I_{yz} \\ I_{xz} & I_{yz} & I_{zz} \end{bmatrix} \tag{2}$$

Inertia matrix $\boldsymbol{I}$ is represented in the frame F_1 located at the center of mass (see Figure 2). Details of the inertial model and how Kalman Filters are used to achieve the online estimation can be found in (He, 2013). The same method is used for the

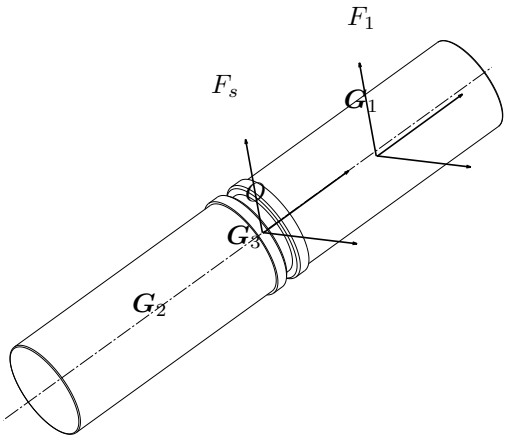

Figure 2: The frame F_1 is located at the center of mass of the upper part of the Bidule object. The frame F_s is located at the center of the force/torque sensor. $\boldsymbol{G}_1$ represents the inertial model of the upper part and $\boldsymbol{G}_2$ that of the bottom part.

bottom part $\boldsymbol{G}_2$. It should be noted that $\boldsymbol{G}_3$ and different coordination transformation need to be handled carefully. We will omit the details in this paper because of limited space. Kubus et al. proposed a recursive approach in (Kubus, Kroger, & M.Wahl, 2008) to solve a similar problem. Although we use an Unscented Kalman Filter instead of Recursive Least Square, the readers can refer to the paper for more discussion on the topic. Once the whole set of inertial parameters are estimated, the inertial forces ($f_{inertia}$ and $\tau_{inertia}$) are simulated and removed from the sensored signals (f_{sensor} and τ_{sensor}), and we obtain contact forces ($f_{contact}$ and $\tau_{contact}$).

$$f_{contact} = f_{sensor} - f_{inertia} \quad (3)$$

$$\tau_{contact} = \tau_{sensor} - \tau_{inertia} \quad (4)$$

The structure of this calculation can be summarized as:
Bidule is designed to learn three aspects of object manipulation for a service robot:

- How to classify events from the rich information coming from the f/t sensor during exchange or when the robot end effector contacts environment, either for human grasp or collision with different obstacles.
- The trajectories for hand-over motions adapted to the mass and types of the manipulated object.
- The force control policies for robot during object exchange with human partner.

In this paper, we focus on the first part, while the learning of the trajectory and of the force control policies will be the subject for future research.

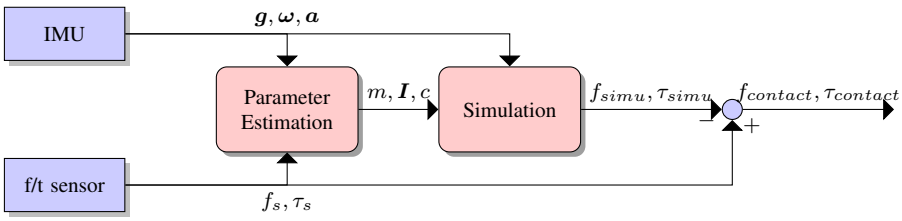

Figure 3: Contact Forces/Torques Computation. The gravitational vector $\boldsymbol{g}$, acceleration $\boldsymbol{a}$ and angular velocity $\boldsymbol{\omega}$ can be computed from an inertial measurement unit (IMU). f_s and τ_s are measured forces/torques vectors. The same strategy can be used for a wrist force sensor on the robot arm to achieve online estimation of the contact forces/torques.

4 Force Signal Monitoring by Classification

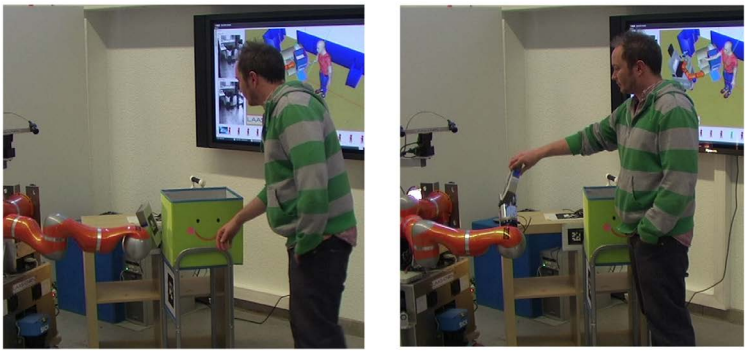

Figure 4: Left: the manipulated object collides with the green box. Right: human takes the object given by the robot.

The control of our robot is centered around a trajectory controller based on Online Trajectory Generation (OTG) (Broquère, Sidobre, & Herrera-Aguilar, 2008) (Kroger & Wahl, 2010) (Broquère, 2011). During the hand-over, several situations concerning the contact forces will occur:

- To give an object to a person, the robot approaches and tracks the exchange point, which is computed in a frame attached to the human partner. When the person grasps the object, the robot detects the event and opens the gripper. If it is still moving, the robot stops its movement and then it retracts the arm along the same path. This enables a dynamic and reactive object exchange.
- During the hand-over motion, the manipulated object can collide with the human hand or with the environment. The human can also fail to grasp the object. For

safety issue, the robot should react differently, depending on the type of collision or failed grasps.

Two such events are shown in Figure 4. Our first objective for learning is to use continuous classification to monitor the force signal history, the previous second for example, to identify what situation it is. We want the robot to be able to use classification to distinguish different contact types and, more importantly, to open the fingers or to stop the motion at the right moment. We define firstly three classes: collision, grasp, and all the rest cases: pure noise, or grasp/collision but not yet the moment to react. In this paper, we limit environment to rigid bodies, such as a table, chair, and other rigid objects in the working space of the robot. The signals would be different collision happened between compliant bodies, and the study for more environment types will be part of our future work.

The examination of the time series of forces/torques shows they depend on the human partner and the manipulated object. For example, a larger object will be handled more slowly and grasped more firmly, so the contact forces should be bigger in magnitude and last longer. Although some simple statistics on the f/t signals could also gain some useful results, we prefer to machine learning techniques to take advantage of the rich time-frequency information in the signals and obtain robust control policies for the robot.

In Figure 5, we see several examples of the forces/torques produced when the object is grasped by a person or during typical collision between Bidule and a table. They show different forms of vibration. We can see that grasp exhibits more variation and collision has a higher-frequencies pattern. For either of the two classes, neither the magnitude nor the duration of the vibration could be easily used to identify the signal. However some characteristics can be used to achieve the classification, which is what we try to extract by machine learning. The choices of techniques are oriented to obtain a computationally efficient and hence fast classifier so it can be run at a high rate, together with other algorithms such as Online Trajectory Generation and online collision checking.

5 Feature Extraction and Learning

5.1 Wavelet Packet Transformation

The contact forces are transient signals, for which wavelet based methods have been established to be a reasonable choice to extract time-frequency information. Comparing to Fourier analysis, wavelets capture not only the frequency information, but also the time localization. The Wavelet Packet Transformation (WPT) used for feature extraction is reported in various work relating to myoelectric signal (Englehart, Hudgins, Parker, & Stevenson, 1999) or underwater acoustic signal (Learned & Willsky, 1995). Wavelet Packet Transformation is an algorithm to decompose discrete signals into subbands with different time-frequency resolutions (Mallat, 2008). Each step of decomposition is implemented as being filtered by a two-channel filter bank, together with downsampling operations. Figure 6 shows an example of a signal of size sixteen

decomposed by a Haar filter bank (A.Jensen & Cour-Harbo, 2001). The original signal is represented at level zero of the tree. At level $j = 1$, the blue part is obtained by lowpass-downsampling operations of the signal, while the pink part is obtained by highpass-downsampling operations. The same computation is then executed on these two signals, decomposing the signal into four subbands (level $j = 2$). The signal is decomposed until $j = 4$, which is the maximum levels J for a signal of size 16. If the

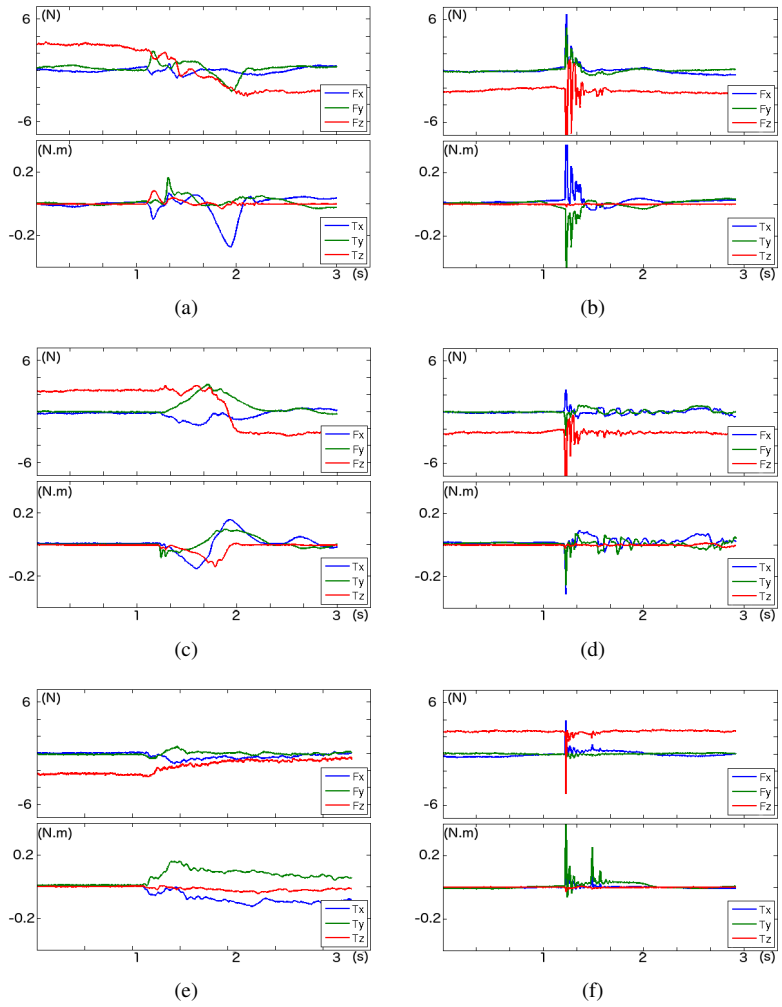

Figure 5: Forces/torques signals during several exchange and collision events. On the left, we see three different object exchanges between two people, when the object mass changes too. On the right, f/t of three different collisions between object and rigid environment happened. The scale for time, force and torque are set to be the same for all the plots.

size of original signal is D, we have $J = \log_2 D$.

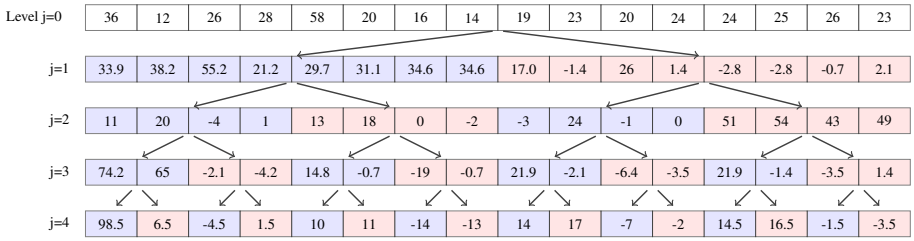

Figure 6: Wavelet Packet Transformation decomposes the original signal recursively into a tree structure, here through the Haar wavelet filter bank. Each subband is decomposed into a high-frequency part (pink) and a low-frequency part (blue).

Notice that in Discrete Wavelet Transformation (DWT), only high frequency part is recursively decomposed. Then it can be seen as one subset of the WPT. The problem with DWT is it may lose the possibility to highlight some features. As reported in (Coifman & Wickerhauser, 1992), only some signals have the information focused in this fixed representation. And (Learned & Willsky, 1995) shows a clear example of a transient signal where some patterns are captured by a WPT, but they will not appear in the results of a DWT.

In our system, as the transformation should be computed in real-time, we choose to implement each step of the wavelet transformation in lifting scheme. The lifting scheme reduces the computation complexity, requires less memory, and maintains always perfect reconstruction. For the implementation details, readers may refer to (Sweldens et al., 1995).

To illustrate the time-frequency pattern of a signal, we computed WPT of a linear chirp signal $y(t) = \sin(k\pi t^2)$ by Daubechies wavelets (*db4*). Then the fifth level is chosen from the tree and ordered by frequency. The results are presented in Figure 7, in which the coordinates of time and frequency is without units because they lost the physical meaning, and magnitude plots the function $\log(1 + x^2(i))$, in which $x(i)$ are the wavelet coefficients in level 5. We can see clearly the pattern of an increasing frequency. The ridges that appear perpendicular to the main diagonal line of increasing frequency are artifacts, which will not influence the results of pattern recognition.

For this signal with a clear increasing frequency, it is easy to illustrate its pattern by constructing a time-frequency plot, but to classify complex and variant contact forces we need tools to help us finding the best pattern representation from the WPT.

5.2 Feature Formation and Selection

From the WPT tree, several kinds of feature representations exist: part of the decomposition coefficients, statistical information of the coefficients, or the energy map (Fatourechi, Mason, Birch, & Ward, 2004) (Birbaumer et al., 2000) (Xue, Zhang, Zheng, & Yan, 2003). The whole coefficients set captures all the in-class variations and noise, which would need a large data set to achieve convergence of the optimization process of learning.

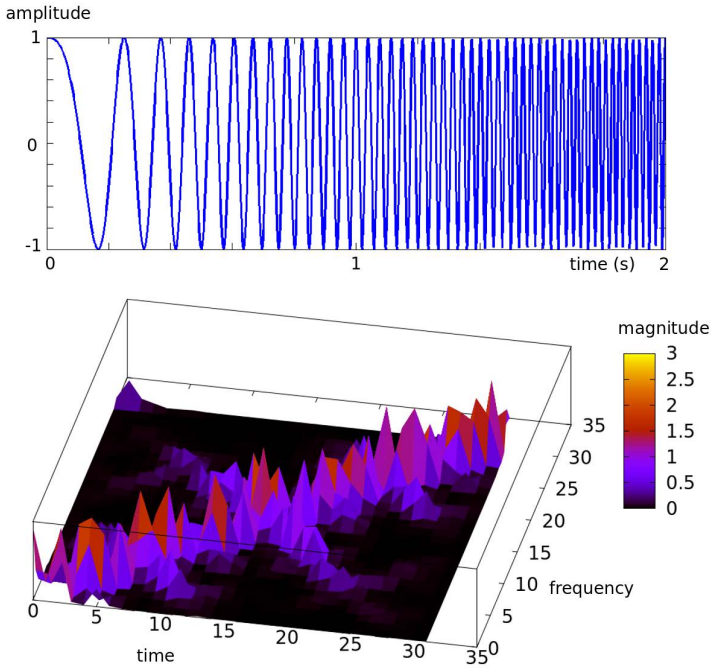

Figure 7: Linear chirp (top) and its time-frequency pattern (bottom), constructed from level 5 of a WPT tree structure. We see that the WPT tree captures the information in time and in frequency.

Feature selection is a critical step to minimize the classification error (Peng, Long, & Ding, 2005). In many applications, increasing the data set would also minimize the classification error, but in our case, building a large data set from manipulations with different candidates and different situations is a tedious task. On the other hand, the classifier will run online at a comparable frequency as the controller, so reduce the dimension of the learned model is also important. Given these reasons, we decide to differentiate in time and in frequency separately by combining a part of the coefficients and the energy map, instead of keeping all the coefficients. As shown in the following, feature selection can reduce significantly the feature size.

The Relative Energy Map is used to capture the frequency information. Each level of the WPT decomposes the signal into a time-frequency representation with different time-frequency precision. For each subband in the tree, an energy value is computed from all the coefficients in the subband. If we name one subband b and its coefficients $x(k)$, then its energy e_b is computed as:

$$e_b = \sum_k \left(x(k)\right)^2 \tag{5}$$

By this definition, e_0, which is computed on the subband S_0 in Figure 8, is the total en-

ergy of the signal, and e_1^L the energy in subband S_1^L. The energy is calculated through the whole tree. Then they are all normalized to the total energy of the signal in the time window, which means:

$$E_b = \frac{e_b}{e_0} \tag{6}$$

For a sample to learn, we write this feature set as $\boldsymbol{E} = \{E_b\}$, which includes the relative energy in all the selected subbands. We notice that a large part of the feature produced by this method are zero, which is no surprise since wavelets produce a sparse representation of the original signal (see (Mallat, 2008) for more details about the sparsity of WPT). We should then choose the most discriminative features from $\boldsymbol{E}$ to further reduce the size of the feature vector.

The energy map is independent of the magnitude and the duration of vibration in the original force signal, and the time information is lost. It can be noted that the relative energy map is already scaled to between 0 and 1.

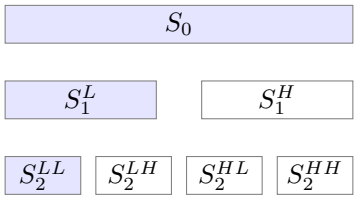

Figure 8: Subbands for the WPT tree of total level 3. L means that the subband has been filtered by a low-pass filter and then downsampled, H means filtered by a high-pass filter and downsampled. The subbands in blue are the low-frequency part at each level.

Coefficients of One Subband are selected to capture the global form of the signal. The objective is twofold: to keep the information of the changing in weight when the receiver starts to hold the exchanged object, and to deduce the right time to open fingers or to react for the robot. The robot should differentiate two signals as shown in Figure 9 where the same signal is shifted in time. We choose the coefficients from the first subband of a level in the WPT tree. It contains information of low frequency part of the signal and with a reduced size. We write this feature set as $\boldsymbol{S}$. In Figure 8, the candidates are in the blue color. Since each level contains such a low frequency subband, the choice of the level is decided by compromising the classification error and the feature size produced. The higher level we choose for this subband, the less it is precise in time. The coefficients are then normalized to between 0 and 1 as the relative energy map.

The choice of the first subband of a level is based on prior knowledge that for signals in all classes of the problem at hand, this subband does indeed capture well the peaks of the original force signals, as shown by Figure 10. For some signals that contain only high frequency components, the choice of subband needs to be made by feature selection algorithms.

Fisher Linear Discriminant Analysis is then used to select features and to reduce further the dimension of the classification model. Fisher-LDA is a tool used for classi-

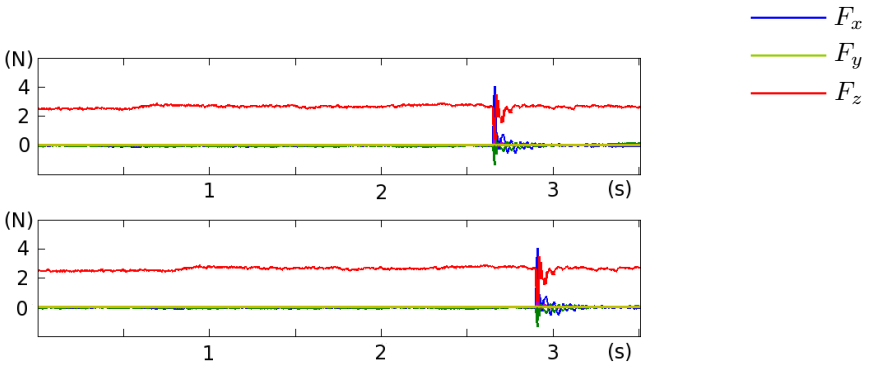

Figure 9: The classifier should be able to make difference between the two signals above to find the right time to react to an event detected by the f/t sensor.

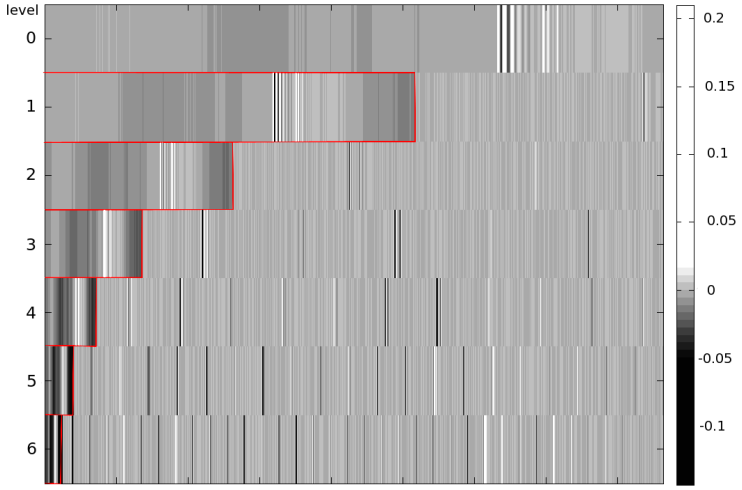

Figure 10: Part of the WPT tree plotted for the signal F ($F = F_x + F_y + F_z$) in Figure 9. The first subbands (highlighted by red rectangle) capture the peak in signal (the peaks are in white color). The WPT is computed with Symlets 5 wavelets (*sym5*). The zeros in the tree show also the sparsity of the WPT. The Unit for horizontal axis is omitted since time measurement unit varies for different levels in the WPT. And level 0 is the original time signal.

fication and dimension reduction of features (Welling, 2005). Detailed discussion for this tool can be found in (Bishop et al., 2006). Fisher-LDA considers finding the best weight $\boldsymbol{w}$ by maximizing the objective:

$$J(\boldsymbol{w}) = \frac{\boldsymbol{w}^T S_B \boldsymbol{w}}{\boldsymbol{w}^T S_W \boldsymbol{w}} \tag{7}$$

where S_B is the "between classes scatter matrix", and S_W is the "within classes scatter matrix" (Welling, 2005). The value of J means the separability of classes for a set or a

subset of features. Here, we use the criterion to select the best features in our feature set of the relative energy map $\boldsymbol{E}$. The criterion is reformulated into definition defined as (8). It is calculated for every feature in $\boldsymbol{E}$ to evaluate the separability measure (Gu, Li, & Han, 2011) of that feature. As WPT produces a sparse representation of the signal, which means many terms in the tree are nearly zero, it is reasonable not to include those features, which are invariant between classes.

$$J = tr(S_W^{-1} S_B) \tag{8}$$

During the object exchange manipulation, the orientations of f/t changes in different situations: the posture of the robot and of people, the exchange positions, and more. Not including orientations for the event detection simplifies the problem. In fact, the f/t are expressed in the local frame of the sensor, which makes the orientations more difficult to use for the classifier. Learning a model with orientations will also be much more complex and produce a model of much higher dimension, resulting in a slower classifier. While the orientations of f/t are excluded from the feature set, the feature set building process can be summarized as:

- The WPT tree representation is built from force F and from torque T, F is computed as $F = ||Fx + Fy + Fz||$, and T is computed as $T = ||Tx + Ty + Tz||$.
- The relative energy map is computed for the WPT.
- It is then combined with a subband from the tree. The subband is also scaled to range from 0 and 1, matching the same as relative energy map.
- Fisher LDA criterion is used to reduce the size of the feature set of energy map $\boldsymbol{E}$ and the level from the subband $\boldsymbol{S}$ selected as a trade-off between the classification accuracy and feature size.

5.3 RVM and Classification

Once the features are well defined, the problem is formulated as classification of multiple-classes. In the previous section, the f/t signals are transformed into the feature space of the energy map and a subband from the WPT tree. If we write the whole feature vector as $\boldsymbol{x}$, then this problem is: given $(\boldsymbol{x}_i, d_i)_{i=1,2,...N}$, a set of N training data where d_i is the class label, how to determine a classifier $y(\boldsymbol{x})$ that correctly classifies the force signals. The Support Vector Machine (SVM) established itself as the state-of-the-art algorithm with strong theoretical foundations for classification and regression (Vapnik, 1999) (Burges, 1998). However, the new Relevance Vector Machines (RVM) approach is really promising, and we choose it for this work. Compared to SVM, RVM has some advantages, as discussed in (Tipping, 2001), which will not be repeated in this paper.

We show how a sparse model is achieved by RVM. For clarity, the simple case of a binary classification problem is discussed, which means $d_i \in \{0, 1\}$. Given a new input vector $\boldsymbol{x}_*$, the probability of its class label is given as:

$$p(d|\boldsymbol{x}_*) = \frac{1}{1 + \exp(-y(\boldsymbol{x}_*))} \tag{9}$$

the RVM classifier function y is given by:

$$y(\boldsymbol{x}) = \sum_{i=1}^{N} w_i K(\boldsymbol{x}_*, \boldsymbol{x}_i) \tag{10}$$

In which, $K(\cdot, \cdot)$ is a kernel function, $\boldsymbol{x}_i (i = 1, 2, 3..., N)$ are the N training data. As discussed in (Tipping, 2001), the parameters w_i in (10) are determined by Bayesian estimation, and a sparse prior is introduced on these parameters, forcing them to be highly concentrated around 0. Then they are computed by maximizing the posterior distribution of the class labels given in the inputs. A very few nonzero terms of w_i means that a very few samples in the training data are used in the classifier function given by (10), achieving a sparse model. Like for SVM, the kernel trick is used to expand the basis functions for $y(\boldsymbol{x})$. In this work, the RBF kernel function is used, which is:

$$K(\boldsymbol{x}_*, \boldsymbol{x}) = \exp(-\frac{||\boldsymbol{x}_* - \boldsymbol{x}||^2}{2\sigma^2}) \tag{11}$$

In which, the optimized $\sigma > 0$ defines the kernel width. The choice of RBF kernel is made by trying different kernels and RBF gave satisfying results. Readers can refer to (Bishop et al., 2006) and (Tipping, 2001) to see how RVM is generalized for multiclass problems, and for information for other kernels. RVM has been successfully applied for fault diagnosis (Widodo et al., 2009), supervised hyperspectral classification (Mianji & Zhang, 2011), and for recovering 3D human body pose by regression (Agarwal & Triggs, 2004).

6 Data Acquisition and Results

6.1 The Experimental Protocol

The experiments are carried out with nine pairs of volunteers, all adults but including both genders. We selected people who have worked around robots and also four pairs who have not had the experience. Three qualitative velocities were chosen: slow, normal and fast and explained to each participant. First, Bidule was presented to volunteers as a precious and fragile object that needs to be handle with care. These exchanges define the slow velocity exchanges. Then the real solidity of Bidule was revealed and they were asked to carry out natural exchanges, namely normal velocity exchanges. Then the volunteers were asked to do fast exchanges.

We defined four different orientations for Bidule, the two vertical ones (antenna up and upside down), one horizontal and one tilted. We did one third of these experiments with an additional mass. Figure 11 presents the seventeen different cases of exchange, while Figure 12 shows one such exchange experiment. Each couple of volunteers performed two times each case of exchange, one as giver and one as receiver. Each record lasts three to five seconds, depending on the speed of object exchange.

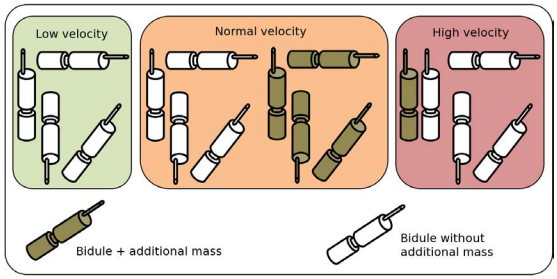

Figure 11: The configurations of Bidule used for the experiments

Figure 12: Two persons equipped with markers and exchanging Bidule

6.2 The Data Set

Firstly the time window is fixed to approximately 1 second because we observed that the slowest manipulation lasts about 1 second, which gives 2048 data points as the acquisition rate is set to 1kHz (1024 for force data points and 1024 data points for torque). By discarding failed data records because of various reasons such as communication failure, 213 experiments for each type of events ("collision" and "grasp") are selected. For class "collision", we recorded data of class collision between Bidule and different environment: human hand, table, bottles, and video tapes. We limit the environment to the working space of the robot, which includes only rigid bodies. Including soft bodies in the "collision" database would change how the classifier identifies events, and how that works on the robot needs further investigation. As we need to model the correct time to release the object for the giver, the samples for class "noise" are simply cut from the data, which could be pure noise, or just signal at different instant from the reaction time, shifted by 0.05, 0.1, and 0.15 second, etc. We used a random process to segment data samples of "noise" from recorded noise signals, with the smallest time difference of 0.05 second. The total data set for training is of size 639. Then 240 data of the three classes are also selected in the same way to test the model.

6.3 Feature Selection Results

In this section, we will discuss the choice of features by some results. Table 1 shows the result of classification with different feature set: the full energy map ($\boldsymbol{E}$), the subband from level 1 $\boldsymbol{S}$, and the two combined. The choice to combine two different feature sets is justified by the results in the classification errors.

Table 1: Error rate for different feature set. RVM with a RBF kernel is used as the classifier

Features	$\boldsymbol{E}$	$\boldsymbol{S}$	$\{\boldsymbol{E}\ \boldsymbol{S}\}$
Error(%)	15.42	21.67	2.5

To reduce the feature size of the relative energy map $\boldsymbol{E}$ and the subband $\boldsymbol{S}$, we did two studies: Firstly, we evaluated $\boldsymbol{E}$ by the Fisher LDA criterion, then we fixed $\boldsymbol{E}$ to evaluate the different choices on $\boldsymbol{S}$ by directly comparing the classification error. Firstly, we calculated the energy map from the WPT until level 6, which produces a total of 126 features for force and 126 for torque. The relative energy of level 0 (original signal) is omitted since it is 1 for all instances. We examine the separability J of the relative energy map feature set $\boldsymbol{E}$. The results can be seen in Figure 13, here for the forces F. Several terms in the feature set dominate the discriminative measure, which enables us to reduce largely the size of the feature set without losing too much the discriminative information of the feature set. The final set of features is chosen from the most discriminating terms from the combination the WPT results of force and of torque.

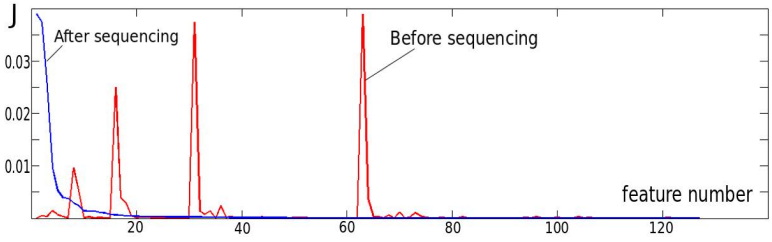

Figure 13: The separability measurement of features in the relative energy map $\boldsymbol{E}$ of forces. J is calculated by Equation (8) through all features in $\boldsymbol{E}$. The zeros in this measurement are largely due to the sparsity of the WPT tree. Similar results are obtained for torques too. The features are sequenced by the separability measurement J in a decreasing order.

For the choice of the level from which to extract the low frequency subband, we use RVM with RBF kernel and compare directly the classification error rate. During this study the energy map is reduced to the first 13 most discriminative features. Firstly we choose $\boldsymbol{S}$ at the first level, then evaluate the classification error. Then we evaluate at level 2 and until that the error rate of classification increased significantly at level 6.

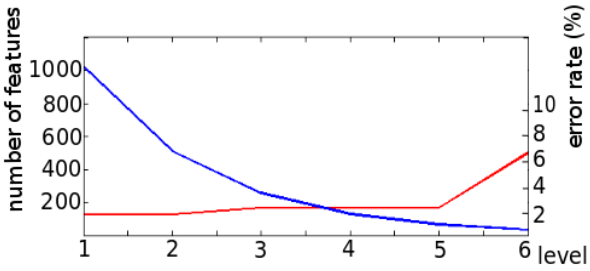

Figure 14: The trade-off between feature size (blue curve) and classification error (red curve). The small feature size means a faster model for online prediction. Level 5 is chosen as it gives a satisfying balance between number of features and error rate.

It can be explained by the losing of time precision in the higher level of the WPT tree. The subband is fixed to level 5 to keep error rate low with low number of features.

Table 2: For this application, RVM produces a much sparser model than SVM, and a comparable classification accuracy.

	Dimension	Accuracy(%)
SVM	151	97.92
RVM	9	97.5

By this study, we finally chose the first 13 features out of 252 of the relative energy map $\boldsymbol{E}$. The subband of level 5 gives 64 features. After the dimension reduction, a classification accuracy rate of 97.5% is obtained, with a compact model having dimension of 9 (the nonzero weights in RVM), while feature size is 77. When the whole WPT tree is used directly to train a RVM, the learning does not converge because of the in-class variations and due to the small size of the training data set, and the whole WPT tree decomposed until level 6 is of size 12288 (each level has 1024 elements for forces and 1024 elements for torques).

6.4 Comparison to SVM

When the same feature set is used for a SVM, it gives a similar classification accuracy. As shown in Table 2, RVM produces a much sparser model (hence faster classification). In the table, the dimensions are the number of Support Vectors or of Relevance Vectors. Since we want to run the classifier online at a comparable speed of the controller with other resource consumming computations, reduced complexity in model is important. Notice that only the used features but not the whole WPT tree need to be computed for online classification. The results for SVM is obtained by running the *libsvm* (Chang & Lin, 2011) (RBF kernel).

The 2.5% classification error happens all when the classifier gives label "collision" when the object is grasped by a person. In this case the robot does not open the gripper

when the object is grasped. Although we believe that 2.5% error rate is acceptable, it will be interesting to investigate how we can improve this in the future.

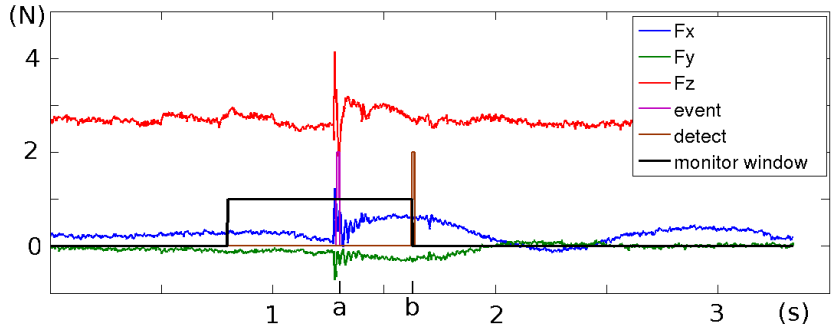

Figure 15: Time delay between the moment when the object comes in contact (shown by "event", and classified as type "collison") and the moment when the robot reacts (shown as "detect", and the reaction is "stop"). The event happens at time a, and the robot reacts at time b. At time b, the system monitors the past 1 second of f/t. This time window that the system monitors is illustrated by the black line.

6.5 Firsts Results with a Robot

The classifier is implemented on the robot for the wrist f/t sensor, which is capable of using the learned model from human experience. The classifier runs at 50Hz, together with other software of perception and planning on the robot. Figure 15 demonstrates the interaction forces and the time delay before the robot react. For this experiment, the object was held by the robot, and a person grasped the object, but not firmly. The event given by the classifier is not "grasp" but "collision", showing the ability to tell if the object is properly grasped. The figure shows the time delay between the grasp event and the time for the robot to react (here, is not to open the gripper but stop the motion, since "collision" is detected, instead of "grasp"), with detection by force signals.

The time delay is normally less than half a second between the event happening and the reaction, with an average of 0.37 seconds. So the choice of a one second observation window seems adequate. One important aspect is that the result does not show the fastest speed the classifier can detect the event, but the right moment to react. This delay is learned by the model, which is decided by the instances acquired by human to human manipulations. It is possible that volunteers tend to exchange Bidule slower than how they do in daily life with familiar objects, but we do not have strong results about this hypothesis. The classifier, on the other hand, can achieve faster detection if only fast training data is selected. We achieved a model which gives 0.2 second reaction by a smaller set of selected fast data, but we decide that the reaction speed should be determined by user study instead of hand selection of training data.

We would like to mention that external force monitoring is implemented on the joint space when collision detection is needed for safety issues, so this reaction time does not introduce safety issue for the robot.

First manipulations between robot and people have been carried out with promising results. Figure 16 shows how the software, from signal processing to classification, are used for manipulations. During this manipulation, the robot decides to open the gripper. A user study of this approach to see how it can improve the quality of object exchange for human users in interactive manipulation is still to finish. The user study will include many aspects, such as human preference for the speed of reaction of the robot. Another example would be to compare the false negative and false positive for grasp detection and see which one has the greater influence on user's experience.

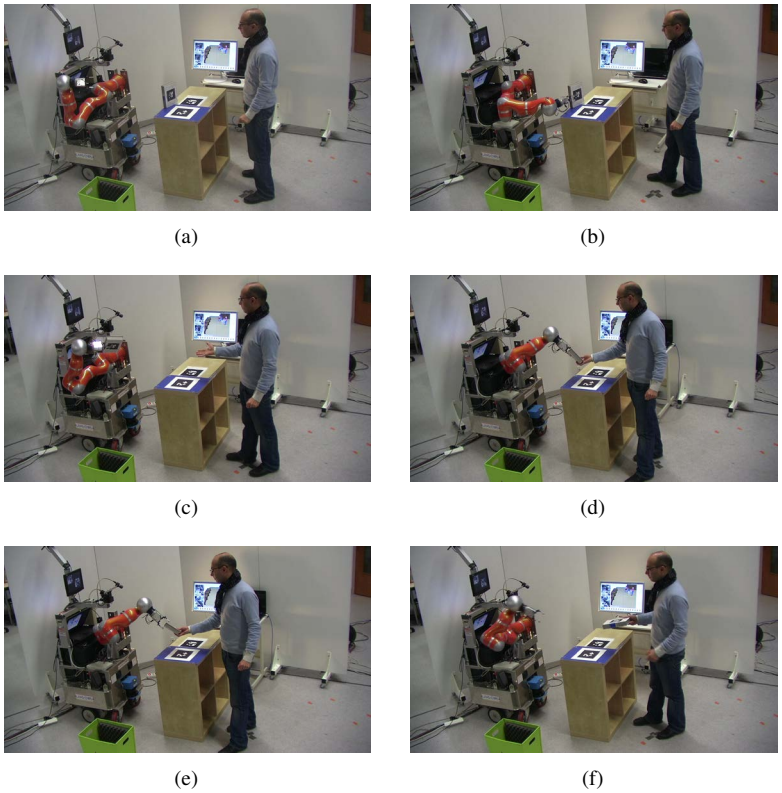

(a) (b) (c) (d) (e) (f)

Figure 16: Software tested during manipulation. (a): Robot Jido, the human partner and objects to manipulate. (b): The robot decides to take the object on the table. (c): The person asks for the object. (d): Robot gives the object to him, and he takes the object. (e): Detecting that the object is taken by the person, the robot opens the gripper. (f): Object exchange finished with success.

7 Conclusion and Future Work

The device proposed to teach the robot how to exchange object like humans is very promising as rich information can be extracted. Force signal classification is studied in this paper. Wavelet Packet Transformation is chosen, from which the energy map and a subband are used to extract the features, and Fisher Linear Discriminant Criterion is used to reduce the dimension of the feature set. Furthermore, the Relevance Vector Machine is employed as classifier because it produces a sparse model. Some results for feature selection and for classification are shown. It can be noted that by constructing a classifier, robust control policies can be achieved with no thresholds to choose by trial and error, which becomes especially difficult when more classes should be considered.

Our experimental device called Bidule has been designed to learn more than what we discussed in this paper, like force control policies during exchange and the movements. Those topics deserve further research and another paper to discuss. For the classification problem, more classes can be added to make a difference between the collisions (soft surface against hard surface), or separate more on the different grasp types. On the other hand, the user study about the event detection is the next work to finish. We need also to investigate the possibilities of using the same set of classification techniques for other manipulations, like putting objects on a table or grasping a handle. At the end, we want to mention that the collision detection by f/t sensor is also to be used for other tasks, such as for the robot to put properly an object on the table. For example, touching of an object with a table by its bottom surface of by an edge would surely produce different patterns on the force signals. And in this case, it would be reasonable to include the torques into the feature set too. With these new methods discussed in this paper to build compact and efficient models, online classification can improve many aspects of the robotic manipulations.

Acknowledgements

This work has been supported by the European Community's Seventh Framework Program FP7/2007-2013 SAPHARI under grant agreement no. 287513 and by the French National Research Agency project ANR-10-CORD-0025 ICARO.

References

Agarwal, A., & Triggs, B. (2004). 3d human pose from silhouettes by relevance vector regression. In *Computer vision and pattern recognition, 2004. cvpr 2004. proceedings of the 2004 ieee computer society conference on* (Vol. 2, pp. II–882).

Aggarwal, P., Dutta, A., & Bhattacharya, B. (2007). Cooperation between a 4 DOF robotic hand and a human for carrying an object together. In *Sice, 2007 annual conference* (pp. 2354–2359).

A.Jensen, & Cour-Harbo, A. (2001). *Ripples in mathematics*. Springer.

Birbaumer, N., Kubler, A., Ghanayim, N., Hinterberger, T., Perelmouter, J., Kaiser, J., ... Flor, H. (2000). The thought translation device (ttd) for completely paralyzed patients. *Rehabilitation Engineering, IEEE Transactions on*, *8*(2), 190–193.

Bishop, C. M., et al. (2006). *Pattern recognition and machine learning* (Vol. 4) (No. 4). springer New York.

Broquère, X. (2011). *Planification de trajectoire pour la manipulation d'objets et l'interaction homme-robot*. Unpublished doctoral dissertation, LAAS-CNRS and Université de Toulouse, Paul Sabatier.

Broquère, X., Sidobre, D., & Herrera-Aguilar, I. (2008). Soft motion trajectory planner for service manipulator robot. In *Ieee/rsj international conference on intelligent robots and systems.*

Burges, C. J. (1998). A tutorial on support vector machines for pattern recognition. *Data mining and knowledge discovery*, *2*(2), 121–167.

Chan, W. P., Parker, C. A., Van der Loos, H. M., & Croft, E. A. (2013). A human-inspired object handover controller. *The International Journal of Robotics Research*, *32*(8), 971–983.

Chang, C.-C., & Lin, C.-J. (2011). Libsvm: a library for support vector machines. *ACM Transactions on Intelligent Systems and Technology (TIST)*, *2*(3), 27.

Coifman, R. R., & Wickerhauser, M. V. (1992). Entropy-based algorithms for best basis selection. *Information Theory, IEEE Transactions on*, *38*(2), 713–718.

Englehart, K., Hudgins, B., Parker, P. A., & Stevenson, M. (1999). Classification of the myoelectric signal using time-frequency based representations. *Medical engineering & physics*, *21*(6), 431–438.

Fatourechi, M., Mason, S., Birch, G., & Ward, R. (2004). A wavelet-based approach for the extraction of event related potentials from eeg. In *Acoustics, speech, and signal processing, 2004. proceedings.(icassp'04). ieee international conference on* (Vol. 2, pp. ii–737).

Gu, Q., Li, Z., & Han, J. (2011). Linear discriminant dimensionality reduction. *Machine Learning and Knowledge Discovery in Databases*, 549–564.

He, W. (2013). *Reactive control and sensor fusion for mobile manipulators in human robot interaction*. Unpublished doctoral dissertation, LAAS-CNRS and Université de Toulouse, Paul Sabatier.

Kim, I., Nakazawa, N., & Inooka, H. (2002). Control of a robot hand emulating human's hand-over motion. *Mechatronics*, *12*(1), 55–69.

Kroger, T., & Wahl, F. M. (2010). Online trajectory generation: basic concepts for instantaneous reactions to unforeseen events. *Robotics, IEEE Transactions on*, *26*(1), 94–111.

Kubus, D., Kroger, T., & M.Wahl, F. (2008). Improving force control performance by computational elimination of non-contact forces/torques. In *Ieee international conference on robotics and automation.*

Learned, R. E., & Willsky, A. S. (1995). A wavelet packet approach to transient signal classification. *Applied and Computational Harmonic Analysis*, *2*(3), 265–278.

Mallat, S. (2008). *A wavelet tour of signal processing: The sparse way*.

Mianji, F. A., & Zhang, Y. (2011). Robust hyperspectral classification using relevance vector machine. *Geoscience and Remote Sensing, IEEE Transactions on*, *49*(6), 2100–2112.

Nagata, K., Oosaki, Y., Kakikura, M., & Tsukune, H. (1998). Delivery by hand between human and robot based on fingertipforce-torque information. In *1998 ieee/rsj international conference on intelligent robots and systems, 1998. proceedings.* (Vol. 2).

Nakasawa, N., Kim, I.-H., Inooka, H., & Ikeura, R. (1999). Force control of a robot hand Emulating human's grasping Motion. In *Systems, man, and cybernetics, 1999. ieee smc '99 conference proceedings. 1999 ieee international conference on* (Vol. 6, p. 774-779 vol.6). doi: 10.1109/ICSMC.1999.816649

Nakazawa, N., Kim, I., Inooka, H., & Ikeura, R. (2001). Force control of a robot gripper based on human grasping schemes. *Control Engineering Practice*, *9*(7), 735–742.

Peng, H., Long, F., & Ding, C. (2005). Feature selection based on mutual information criteria of max-dependency, max-relevance, and min-redundancy. *Pattern Analysis and Machine Intelligence, IEEE Transactions on*, *27*(8), 1226–1238.

Rehman, A., Gao, Y., Wang, J., & Wang, Z. (2012). Image classification based on complex wavelet structural similarity. *Signal Processing: Image Communication*.

Romano, J. M., Hsiao, K., Niemeyer, G., Chitta, S., & Kuchenbecker, K. J. (2011). Human-inspired robotic grasp control with tactile sensing. *Robotics, IEEE Transactions on*, *27*(6), 1067–1079.

Sato, M., Poupyrev, I., & Harrison, C. (2012). Touche: enhancing touch interaction on humans, screens, liquids, and everyday objects. In *Proceedings of the 2012 acm annual conference on human factors in computing systems* (pp. 483–492).

Sidobre, D., Broquère, X., Mainprice, J., Burattini, E., Finzi, A., Rossi, S., & Staffa, M. (2012). Humanrobot interaction. In B. Siciliano (Ed.), *Advanced bimanual manipulation* (Vol. 80, p. 123-172). Springer Berlin Heidelberg. Retrieved from `http://dx.doi.org/10.1007/978-3-642-29041-1_3` doi: 10.1007/978-3-642-29041-1_3

Sweldens, W., et al. (1995). The lifting scheme: A new philosophy in biorthogonal wavelet constructions. *Wavelet Applications in Signal and Image Processing*, *3*, 68–79.

Takubo, T., Arai, H., Hayashibara, Y., & Tanie, K. (2002). Human-robot cooperative manipulation using a virtual nonholonomic constraint. *International Journal of Robotics Research*, *21*(5), 541–553.

Tipping, M. E. (2001). Sparse bayesian learning and the relevance vector machine. *The Journal of Machine Learning Research*, *1*, 211–244.

Vapnik, V. (1999). *The nature of statistical learning theory*. springer.

Welling, M. (2005). Fisher linear discriminant analysis. *Department of Computer Science, University of Toronto*.

Widodo, A., Kim, E. Y., Son, J.-D., Yang, B.-S., Tan, A. C., Gu, D.-S., ... Mathew, J. (2009). Fault diagnosis of low speed bearing based on relevance vector machine and support vector machine. *Expert Systems with Applications*, *36*(3), 7252–7261.

Xue, J.-Z., Zhang, H., Zheng, C.-X., & Yan, X.-G. (2003). Wavelet packet transform for feature extraction of eeg during mental tasks. In *Machine learning and cybernetics, 2003 international conference on* (Vol. 1, pp. 360–363).

Authors' names and contact information: Wuwei He and Daniel Sidobre CNRS, LAAS, 7 avenue du colonel Roche, F-31400 Toulouse, France; and Univ de Toulouse; UPS, LAAS; F-31400 Toulouse, France. Email: wuwei.he@laas.fr and daniel.sidobre@laas.fr.